Supplementary figure legends

Supplementary Figure S1. PRMT5 expression in AML. (A) Analysis of PRMT5 expression in the TCGA AML Cohort to determine the variation among different AML subsets. Associated clinical data were used to group patients based on the reported cytogenetic abnormalities (table on the right). The bar plot shows the average of the normalized read counts for all samples in each cytogenetic group. Error bars represent the standard error of the expression. Welch's ttest was performed to compare the expression between each cytogenetic group. No comparison achieved significance. (B) PRMT5 transcript levels in AML samples (total n=10: primary patients' samples; n=4 and patient-derived cell lines; n=6) when compared to normal bone marrow (n=4).

Supplementary Figure S2. Activities of mutant PRMT5 in AML. (A) Symmetric dimethylation of arginine 3 of histone H4 induced by wild-type full-length PRMT5, PRMT5 (WT), or a catalytically inactive mutant form (G367A/R368A); PRMT5 (Mut), in THP-1 AML cells. (B) Colony forming assay in THP-1 cells transduced with either PRMT5 (WT) or PRMT5 (Mut) when compared to negative control (EV transduced cells). Number of colonies was scored after 10 days

Supplementary Figure S3. (A) HLCL-61 binding to PRMT5 active site. HLCL-61 is represented as gray ball-and-stick model; BLL-1 as thin blue stick model; and Phe327, Trp579 and Lys333 as thinner stick models. PRMT5 catalytic site is depicted as ribbon model. Insets are chemical structures of BLL-1 and HLCL-61. (B) In vitro enzyme assay measuring methylase activity in presence of PRMT5 inhibitor compounds and different

PRMT enzymes including type I PRMT1 and 4 and type II PRMT7. HLCL-61 shown by arrow was most potent in inhibiting enzymatic activity of PRMT5. PRMT5 inhibitors were not effective towards PRMT1, PRMT4 and PRMT7 enzymatic potential.

Supplementary Figure S4. PRMT5 inhibition in different AML cell lines and patient samples. (A) Dose-dependent reduction in cell viability in different AML cell lines and blasts following PRMT5 inhibition with HLCL-61. IC_{50} values of these HLCL-61-treated AML cell lines and patient blasts is provided in the table on the right. MTS assay was used to measure cell viability after 48 hours incubation of cells with increasing doses of HLCL-61. (B-D) Dose-dependent decrease in cell viability following PRMT5 inhibitor treatment of three AML cell lines harboring fusion proteins; Kasumi-1 [t(8;21); AML1/ETO], NB4 [t(15;17); PML/RARA] and ME-1 [inv(16);CBFB/MYH11]. (E) Growth curve assay in Kasumi-1 cell transduced with either PRMT5 overexpression or EV negative control. Cells were counted using Trypan Blue exclusion method over time. (F) Colony forming assay in Kasumi-1 cells overexpressing PRMT5 compared to EV negative control cells. (G) PRMT5 inhibition in Kasumi-1 cells followed by significant reduction in number of colonies formed by Kasumi-1 cells when exposed to HLCL-61. (H) Dose-dependent increase in surface expression of CD11b in Kasumi-1 cells incubated with PRMT5 inhibitor for 48hrs. (I) AnnexinV/PI expression in Kasumi-1 cells treated with 25 and 50μM of HLCL-61 to inhibit PRMT5. Cells were analyzed by FACS after 48hrs incubation with the compound.

Supplementary Figure S5. Depiction of ChIP-seq data from lymphoma cells probed with anti-PRMT5 and anti-dimethylated histone H3 showing a >10 fold enrichment of methylated histones at promoter of miR-29b when compared to negative IgG control.

We have performed ChIP-Seq on chromatin collected from a mantle cell lymphoma (Jeko), and two diffuse large B cell lymphoma (SUDHL-2 and Pfieffer) cell lines using antisera specific for H3R8(me2) and a control IgG antisera. The figure is illustrating the enrichment of H3R8me2 across 7KB span proximal to miR29A and miR29B1 (-5KB upstream promoter region and the first 3 KB of the UTR).

Supplementary Figure S6. MiR-29b and Sp1 relationship with PRMT5. (A) Overexpression of miR-29b in MV4-11 cells which has minimal endogenous miR-29b using miR-29b/mimic. The western blot is measuring Sp1 expression 48hrs following miR-29b overexpression (B) Knockdown of miR-29b in Kasumi-1 AML cell line (with high basal levels of miR-29b) using miR-29b/LNA. Western blotting was used to measure Sp1 levels after 48hrs following transient transfection of the cells. (C) Knockdown of Sp1 in AML cells (THP-1) using electroporation and siRNA specific for Sp1. Both mRNA and protein levels were measured after 48hrs of transfection. (D) miR-29b transcript levels (pri-miR-29b) in THP-1 cells following Sp1 knockdown measured using qPCR and compared to scramble (sc) transfected control cells. (E) Western blotting showing upregulation of PRMT5 and subsequently Sp1 in THP-1 cells transduced with either PRMT5 overexpression or EV negative control construct. (F) miR-29b transcript levels (pri-miR-29b) in PRMT5-overexpressing THP-1 cells following knockdown of Sp1. Sp1 siRNA and electroporation was used to knockdown the gene

and mRNA levels were measured 48hrs post transfection. (G) miR-29b transcript levels (pri-miR-29b) in MV4-11 cells treated with HLCL-61 to inhibit PRMT5, with or without an excess of Sp1. MiR -29b expression was measured within 48hrs of treatment.

Supplementary Figure S7. Information for predicted promoter regions of FLT3 and miR-29b and list of primers to amplify predicted transcription factor binding sites (~200bp amplification product) at these regions used in ChIP experiments.

Supplementary Figure S8. RNA-seq analysis following PRMT5 knockdown in AML cells. (A) Upregulation of pri-miR-29b transcript expression in MV4-11 cells subjected to PRMT5 downregulation (shPRMT5) compared to scrambled control (scr) measured by raw exon read values. (B) Transcript levels of pri-miR-29b validated by qPCR in total RNA of sequenced samples. (C) Measurements of raw exon reads for FLT3 in PRMT5 knockdown and control samples. (D) Western blot analysis of lysates (RIPA) prepared from sequenced shPRMT5 and scr control. Protein levels of miR-29b targets: DNMT1, DNMT3A, DNMT3B and CDK6 in addition to Sp1 were detected following PRMT5 knockdown. (E and F) DAVID functional pathway analysis of the differentially expressed genes between shPRMT5 and control samples as determined by RNA-seq analysis.

Supplementary data:

Supplementary Table S1. Cytogenetic/molecular characteristics of the AML samples (primary patient blasts and cell lines) used in this study.

Sample	Cytogenetic/molecular feature
Patient #1	FLT3-ITD, $NPM1^{mut}$, CEBPA-WT
Patient #2	FLT3-ITD, NPM1-WT, CEBPA-WT
Patient #3	FLT3-WT, NPM1-WT, CEBPA-WT
Patient #4	FLT3-WT, $NPM1^{mut}$, CEBPA-WT
MV4-11	FLT3-ITD, MLL/AF4
THP-1	FLT3-WT, t(9;11)(p22;q23), MLL/AF9
MOLM13	FLT3-ITD+
Kasumi-1	KIT^{mut} (Asn822Lys), AML1/ETO
OCI-AML3	$NPM1^{mut}$, DNMT3A R882C
KG-1	P53 mutation

Supplementary Figure S1

A

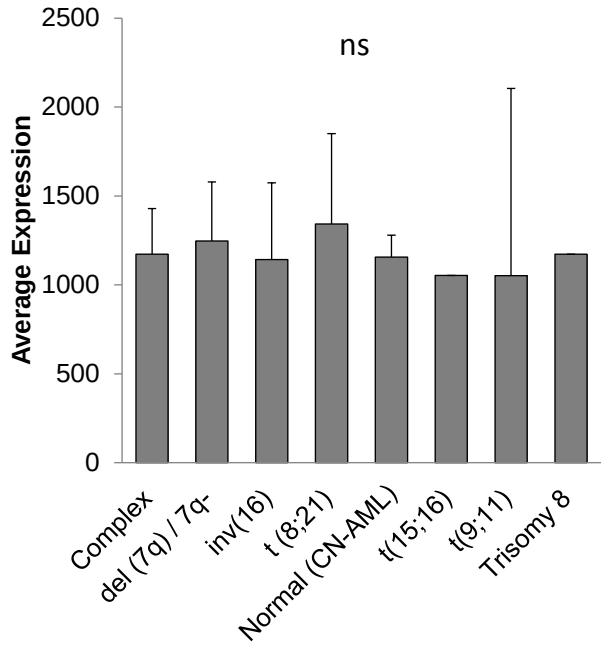

Description	Cytogenetic types
complex; defined as having greater than or equal to 3 distinct abnormalities	Complex|del (5q) / 5q- Complex|del (5q) / 5q-|del (7q) / 7q- Complex|del (5q) / 5q-|del (7q) / 7q-|Trisomy 8 Complex|del (5q) / 5q-|Trisomy 8 Complex|del (7q) / 7q-|Trisomy 8 Complex|Trisomy 8 Normal|Complex Normal|Complex|del (7q) / 7q- Normal|Complex|del (7q) / 7q-|Trisomy 8 Normal|Complex|Trisomy 8
del (7q) / 7q-	del (5q) / 5q- del (5q) / 5q-|del (7q) / 7q- del (7q) / 7q- Normal|del (5q) / 5q-|del (7q) / 7q- Normal|del (7q) / 7q- Normal|del (7q) / 7q-
inv(16)	inv (16) Normal|inv (16)
t (8;21)	t (8;21) Normal|t (8;21)
Normal	Normal (CN-AML)
t(15;16)	|Trisomy 8|t (15;17) Complex|t (15;17) Normal|t (15;17) t (15;17)
t(9;11)	Normal|t (9;11) Normal|del (7q) / 7q-|t (9;11)
Trisomy 8	Trisomy 8

B

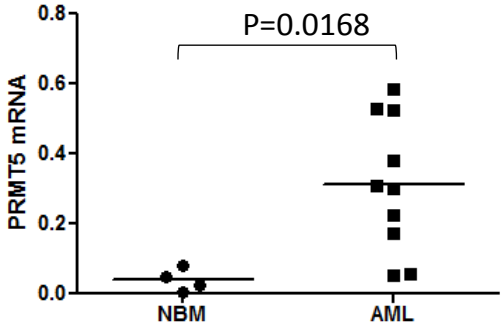

Sample	Cytogenetic/molecular feature
Patient #1	FLT3-ITD, NPM1^{mut}, CEBPA-WT
Patient #2	FLT3-ITD, NPM1-WT, CEBPA-WT
Patient #3	FLT3-WT, NPM1-WT, CEBPA-WT
Patient #4	FLT3-WT, NPM1^{mut}, CEBPA-WT
MV4-11	FLT3-ITD, MLL/AF4
THP-1	FLT3-WT, t(9;11)(p22;q23), MLL/AF9
MOLM13	FLT3-ITD+
Kasumi-1	KIT^{mut} (Asn822Lys), AML1/ETO
OCI-AML3	NPM1^{mut}, DNMT3A R882C
KG-1	P53 mutation

Supplementary Figure S2

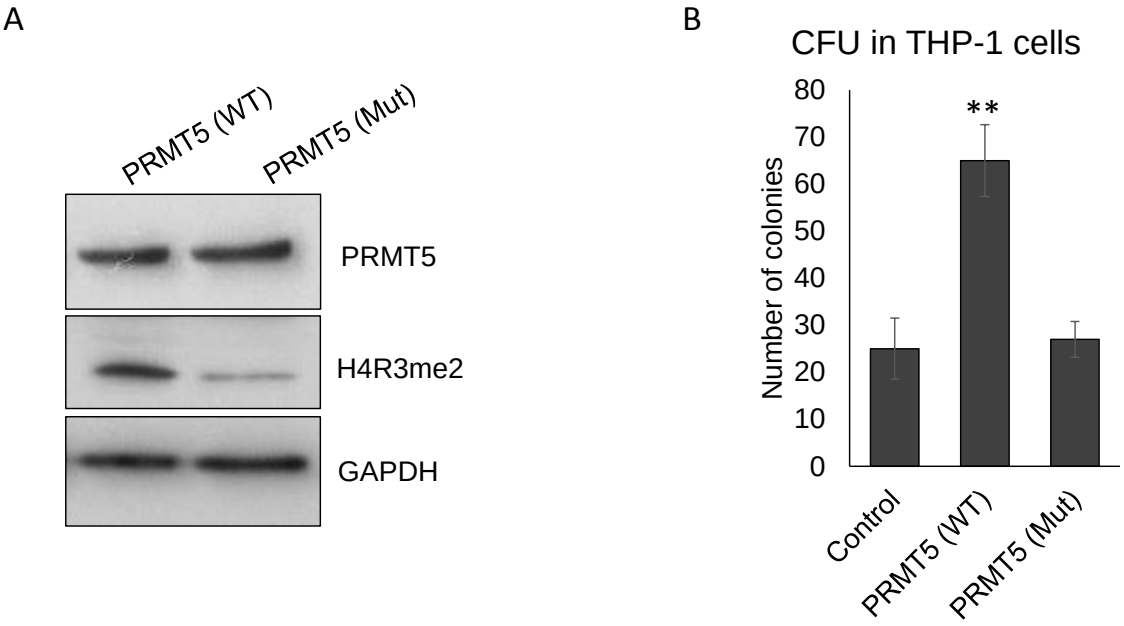

Supplementary Figure S3

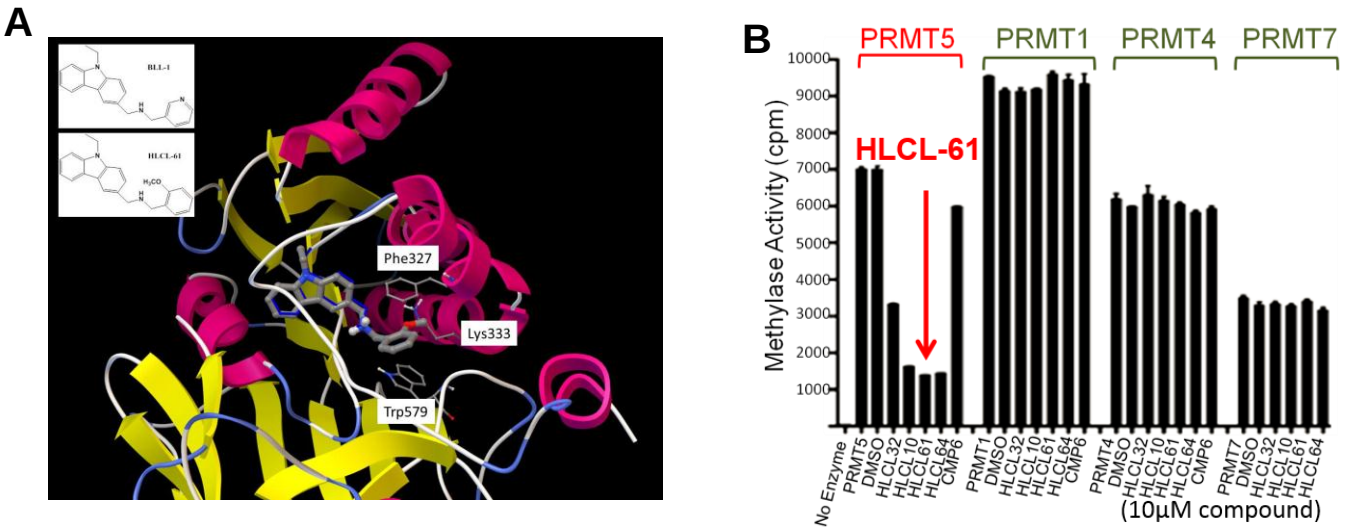

Supplementary Figure S4

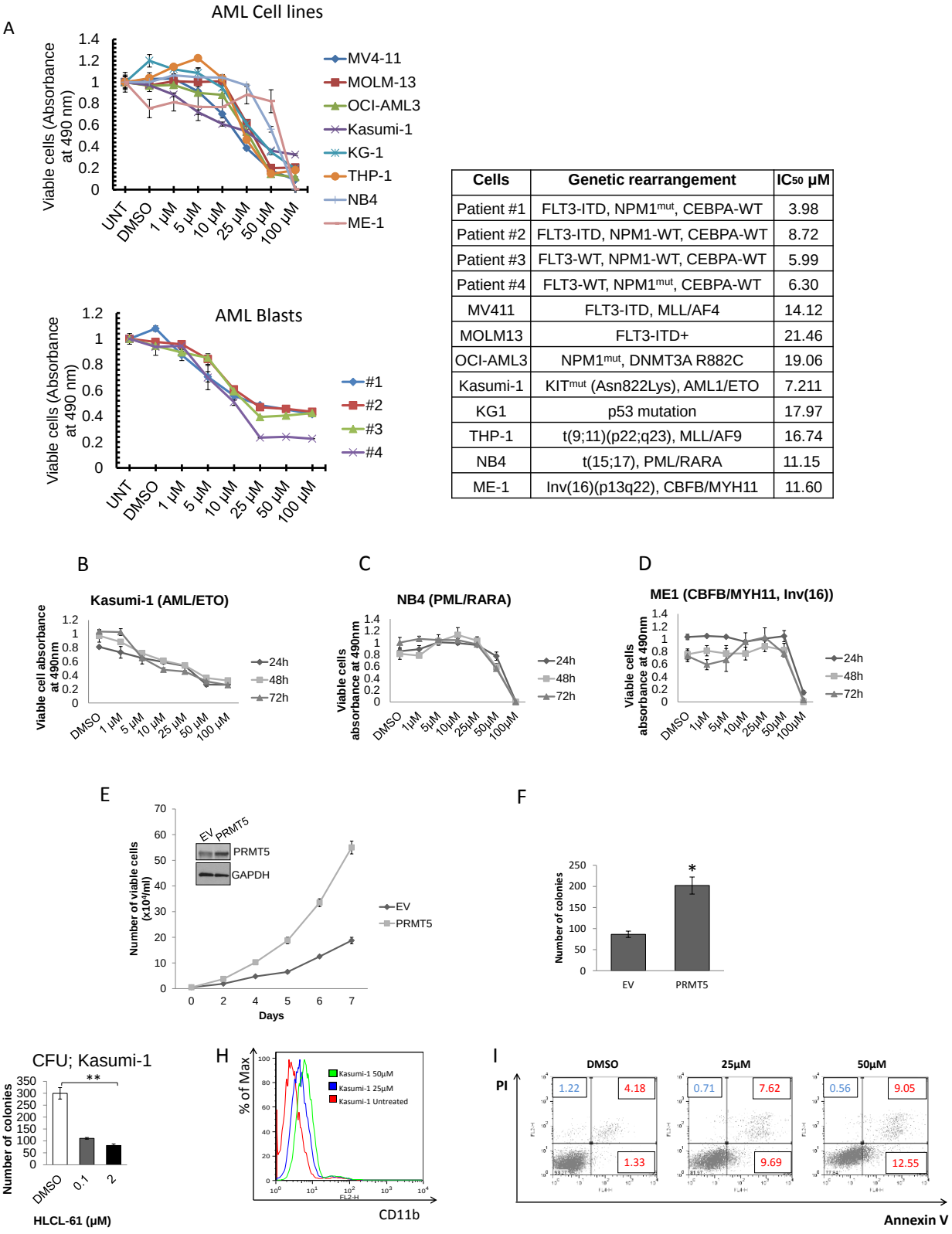

Cells	Genetic rearrangement	IC_{50} µM
Patient #1	FLT3-ITD, $NPM1^{mut}$, CEBPA-WT	3.98
Patient #2	FLT3-ITD, NPM1-WT, CEBPA-WT	8.72
Patient #3	FLT3-WT, NPM1-WT, CEBPA-WT	5.99
Patient #4	FLT3-WT, $NPM1^{mut}$, CEBPA-WT	6.30
MV411	FLT3-ITD, MLL/AF4	14.12
MOLM13	FLT3-ITD+	21.46
OCI-AML3	$NPM1^{mut}$, DNMT3A R882C	19.06
Kasumi-1	KIT^{mut} (Asn822Lys), AML1/ETO	7.211
KG1	p53 mutation	17.97
THP-1	t(9;11)(p22;q23), MLL/AF9	16.74
NB4	t(15;17), PML/RARA	11.15
ME-1	Inv(16)(p13q22), CBFB/MYH11	11.60

Supplementary Figure S5

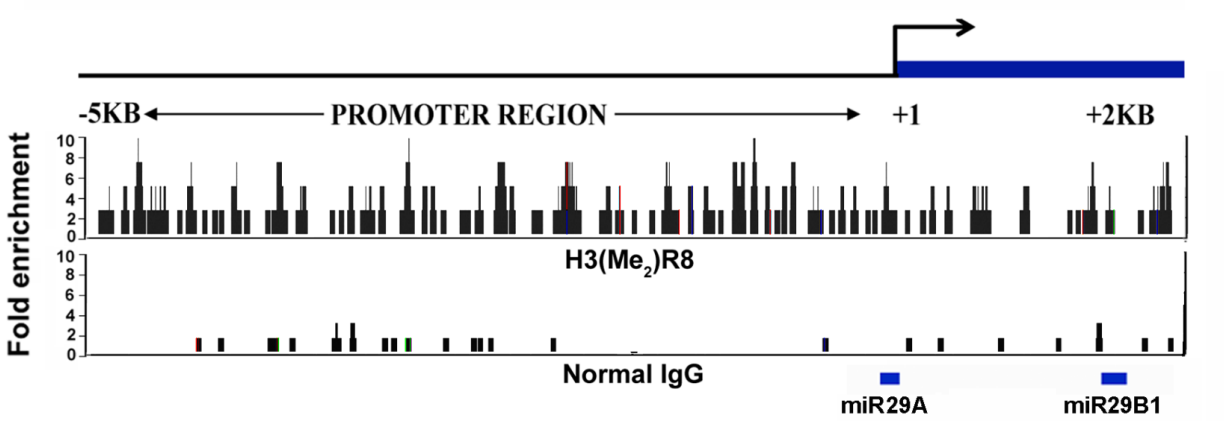

Supplementary Figure S6

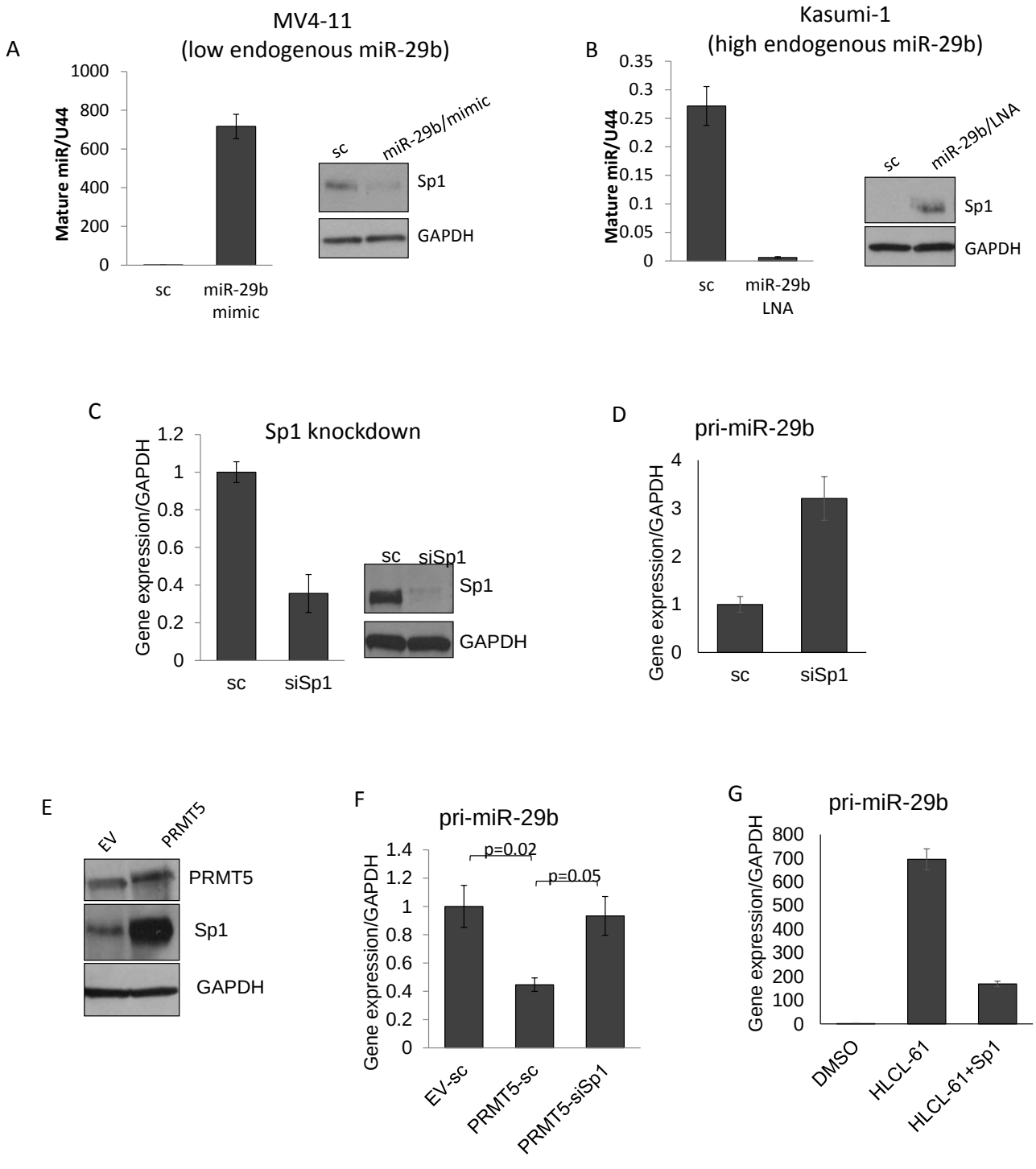

Supplementary Figure S7

FLT3 NG007066 (chr13:4252-5337)

FLT3-ChIP-F: CAGAGTTCGGGGACTCACAG

FLT3-ChIP-R: GAGAGGTTGGGCAGAGCCGAG

miR-29b EU154353 (chr7: 32416-35731)

miR-29b-ChIP-F: TCCTGAGTAGCTGGGATTGC

miR-29b-ChIP-R: CATGCCTGTAGTGAGGCTGA

Supplementary Figure S8

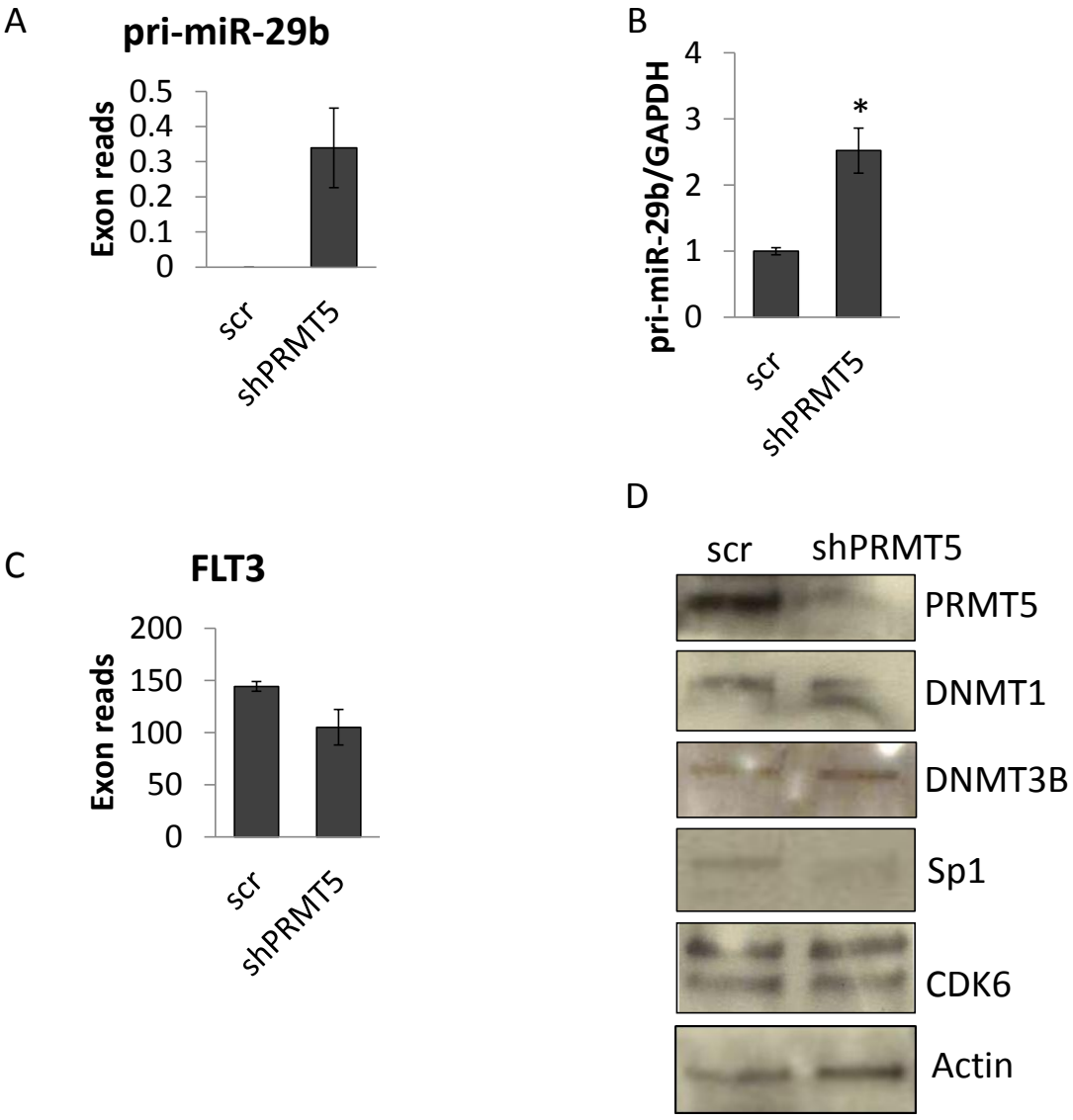

Supplementary Figure S8

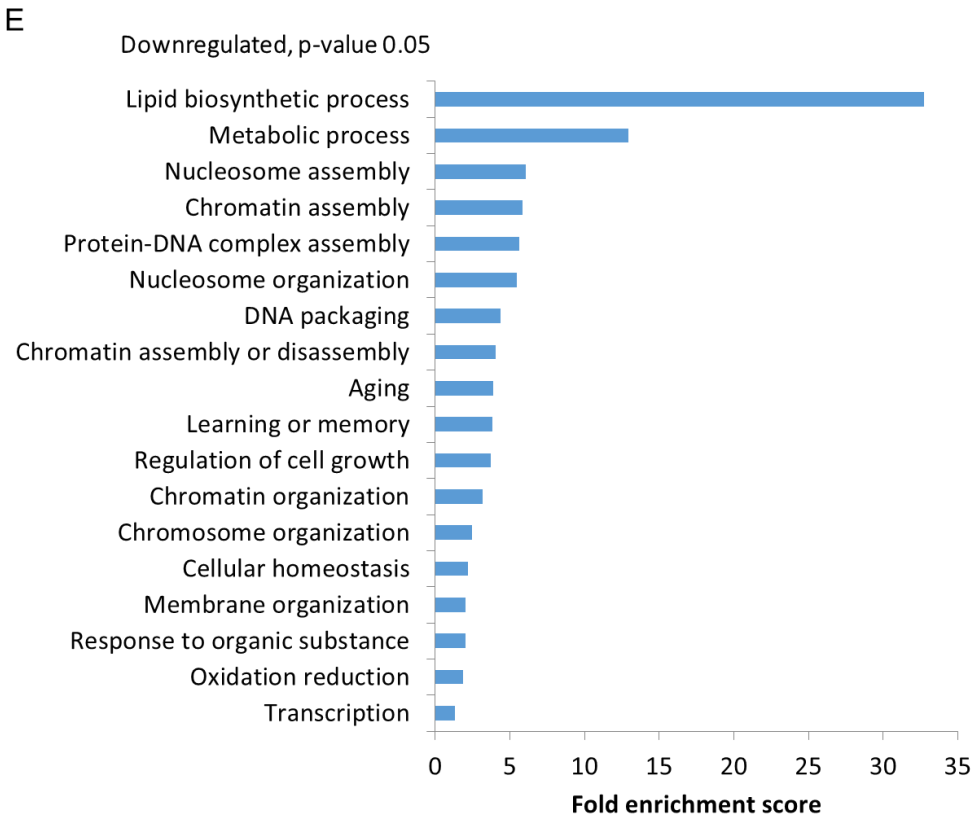

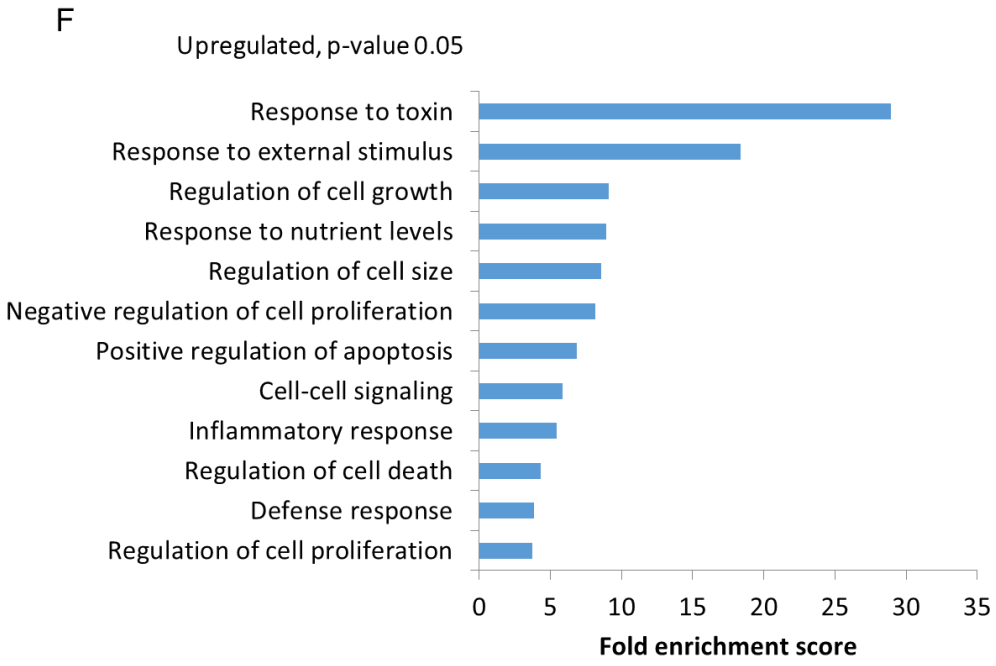

Supplementary Table S2. List of genes significantly up or downregulated in shPRMT5 cells vs. control identified by RNA-seq.

Gene	Chromosome	P-Value	Up or DOWN
CLEC12A	chr12	0.000523	UP
CHAC1	chr15	0.003708	UP
GDF15	chr19	0.020722	UP
SLC7A11	chr4	0.000755	UP
PRG2	chr11	0.01515	UP
NUPR1	chr16	0.018173	UP
STC2	chr5	0.006214	UP
CHI3L1	chr1	0.02243	UP
INHBE	chr12	0.021993	UP
TFAP2C	chr20	0.007323	UP
AGT	chr1	0.009029	UP
IL8	chr4	0.015308	UP
S100P	chr4	0.037481	UP
CTH	chr1	0.008886	UP
FLJ23867	chr1	0.011423	UP
DRAM1	chr12	0.007212	UP
GAL	chr11	0.027371	UP
PSAT1	chr9	0.009376	UP
SLC38A1	chr12	0.014362	UP
NQO1	chr16	0.038021	UP
SNORD48	chr6	0.028028	UP
MFAP4	chr17	0.034342	UP
CYFIP2	chr5	0.007945	UP
CADM1	chr11	0.01812	UP
IGFBP2	chr2	0.038599	UP
C3orf80	chr3	0.045558	UP
C19orf59	chr19	0.01631	UP
ASNS	chr7	0.01387	UP
CCPG1	chr15	0.017411	UP
DYX1C1-CCPG1	chr15	0.018209	UP
CKAP4	chr12	0.015474	UP
PTPN13	chr4	0.022003	UP
HOXA5	chr7	0.047748	Down
MAFK	chr7	0.044053	Down
HMG20B	chr19	0.023189	Down
WHAMM	chr15	0.046223	Down
QPRT	chr16	0.024537	Down
ARHGAP12	chr10	0.031463	Down

HEBP1	chr12	0.030596	Down
TMEM63A	chr1	0.03684	Down
WDR37	chr10	0.037647	Down
RSBN1	chr1	0.034523	Down
BAZ2A	chr12	0.025046	Down
CHRNA7	chr15	0.020174	Down
PCGF1	chr2	0.033103	Down
ZBED6	chr1	0.041538	Down
STARD4-AS1	chr5	0.012426	Down
TMEM55A	chr8	0.031948	Down
C14orf43	chr14	0.047494	Down
UHMK1	chr1	0.029923	Down
KPNA5	chr6	0.044159	Down
ULK4P2	chr15	0.020519	Down
ULK4P1	chr15	0.020525	Down
LOC100507217	chr15	0.022064	Down
PPFIBP1	chr12	0.017127	Down
CALCOCO1	chr12	0.035787	Down
PLEKHA2	chr8	0.017956	Down
DDX3Y	chrY	0.019342	Down
SLC12A4	chr16	0.033233	Down
VAMP4	chr1	0.019274	Down
MVK	chr12	0.043764	Down
ULK4P3	chr15	0.016044	Down
NARF	chr17	0.028011	Down
KLHL15	chrX	0.045227	Down
CLK3	chr15	0.031997	Down
ICAM3	chr19	0.012794	Down
CD37	chr19	0.033582	Down
CCBL1	chr9	0.038929	Down
MAGED2	chrX	0.020137	Down
EZH1	chr17	0.033572	Down
CHRFAM7A	chr15	0.011555	Down
TBC1D3G	chr17	0.048282	Down
SC5DL	chr11	0.039071	Down
NPHP3-ACAD11	chr3	0.036657	Down
MAST3	chr19	0.012444	Down
ING2	chr4	0.034922	Down
SLC9A3	chr5	0.006517	Down
LONRF1	chr8	0.013871	Down
STARD8	chrX	0.01529	Down

MICA	chr6	0.036367	Down
OSBPL2	chr20	0.022726	Down
KDM3A	chr2	0.02496	Down
PTAR1	chr9	0.025429	Down
ATP8B3	chr19	0.010488	Down
ANO8	chr19	0.013372	Down
THBS3	chr1	0.02579	Down
RBM33	chr7	0.022223	Down
AKAP17A	chrX	0.018265	Down
AKAP17A	chrY	0.018269	Down
TMEM41B	chr11	0.030042	Down
MPZ	chr1	0.048989	Down
ABCB7	chrX	0.008361	Down
PPFIA4	chr1	0.046306	Down
CLDND1	chr3	0.014742	Down
ADD3	chr10	0.023941	Down
MEIS1	chr2	0.009528	Down
HMBOX1	chr8	0.015248	Down
C12orf23	chr12	0.028298	Down
FDPS	chr1	0.008528	Down
CLN8	chr8	0.029829	Down
ARHGAP33	chr19	0.007077	Down
HELB	chr12	0.018782	Down
KCTD7	chr7	0.033007	Down
IDI1	chr10	0.021298	Down
RASSF7	chr11	0.015546	Down
ZBTB41	chr1	0.015025	Down
PER1	chr17	0.025959	Down
BNIP3	chr10	0.032975	Down
ZNF467	chr7	0.031235	Down
ZMYM3	chrX	0.012819	Down
BMF	chr15	0.030986	Down
ZNF395	chr8	0.032029	Down
MTHFR	chr1	0.034716	Down
LDLR	chr19	0.013969	Down
C10orf10	chr10	0.018867	Down
RUSC1-AS1	chr1	0.006624	Down
SLC2A14	chr12	0.044534	Down
TRIP10	chr19	0.020066	Down
SERTAD3	chr19	0.014399	Down
GADD45B	chr19	0.032429	Down

DBP	chr19	0.026014	Down
CMTM4	chr16	0.028198	Down
PIK3C2A	chr11	0.018402	Down
LPCAT4	chr15	0.039405	Down
FUT11	chr10	0.021254	Down
H1FX	chr3	0.0153	Down
P4HA1	chr10	0.018556	Down
DHRS1	chr14	0.035153	Down
PLCB3	chr11	0.014296	Down
PLXNA3	chrX	0.017255	Down
FAM8A1	chr6	0.010842	Down
KLC4	chr6	0.014178	Down
SAT1	chrX	0.02258	Down
FAM63B	chr15	0.018033	Down
NDRG1	chr8	0.047308	Down
CCDC144NL	chr17	0.008994	Down
EBP	chrX	0.015635	Down
C18orf25	chr18	0.012294	Down
ARL5B	chr10	0.015645	Down
CLK1	chr2	0.012377	Down
TPM2	chr9	0.021646	Down
KRT8	chr12	0.024646	Down
CLCN6	chr1	0.014992	Down
FAM214B	chr9	0.013083	Down
PTGS1	chr9	0.016377	Down
ZFP36	chr19	0.001716	Down
NR4A1	chr12	0.034555	Down
HMGCR	chr5	0.010847	Down
TNFSF9	chr19	0.0449	Down
ACSF2	chr17	0.017063	Down
ICAM5	chr19	0.006688	Down
SCD	chr10	0.008607	Down
C21orf56	chr21	0.007975	Down
CYP51A1	chr7	0.010776	Down
ZBTB25	chr14	0.02883	Down
MXD1	chr2	0.03425	Down
LOC100128071	chr1	0.031331	Down
PRKAB2	chr1	0.004924	Down
HECA	chr6	0.009644	Down
PNRC1	chr6	0.007306	Down
FCGR2C	chr1	0.00626	Down

NFIL3	chr9	0.027776	Down
TSSK3	chr1	0.019352	Down
CRELD1	chr3	0.017523	Down
SLC30A1	chr1	0.020663	Down
GSDMB	chr17	0.034183	Down
PIM3	chr22	0.009048	Down
YPEL2	chr17	0.010259	Down
SNORA29	chr6	0.044463	Down
ZBTB10	chr8	0.009564	Down
SLC26A6	chr3	0.01012	Down
ABHD4	chr14	0.019235	Down
RHPN1	chr8	0.01799	Down
LSS	chr21	0.002593	Down
FAM193B	chr5	0.0024	Down
DDAH2	chr6	0.003991	Down
LMBR1L	chr12	0.003651	Down
MT1F	chr16	0.016055	Down
PFKFB4	chr3	0.043906	Down
JPH2	chr20	0.00072	Down
FDFT1	chr8	0.003848	Down
GNG7	chr19	0.004161	Down
CERCAM	chr9	0.025483	Down
RAB3A	chr19	0.008062	Down
SPP1	chr4	0.035521	Down
GBP2	chr1	0.005702	Down
SQLE	chr8	0.004866	Down
ZBTB43	chr9	0.011595	Down
SAMD8	chr10	0.005449	Down
TNNT1	chr19	0.03292	Down
GGT7	chr20	0.011899	Down
MVD	chr16	0.006392	Down
SNORD59A	chr12	0.015334	Down
FEM1C	chr5	0.004087	Down
TBC1D30	chr12	0.020218	Down
KLF6	chr10	0.004265	Down
CDK18	chr1	0.036398	Down
LSP1	chr11	0.005661	Down
FADS3	chr11	0.049763	Down
KLHL28	chr14	0.004343	Down
CKB	chr14	0.006102	Down
PHF1	chr6	0.002379	Down

SGK1	chr6	0.006058	Down
INSIG1	chr7	0.002511	Down
ANKRD37	chr4	0.004132	Down
SNORD21	chr1	0.015102	Down
MT1E	chr16	0.006633	Down
TXNIP	chr1	0.009527	Down
FCGR2B	chr1	0.001985	Down
CSRNP1	chr3	0.001625	Down
HSD17B7P2	chr10	0.002851	Down
HSD17B7	chr1	0.002503	Down
RRAS	chr19	0.002396	Down
RAB26	chr16	0.02717	Down
H1F0	chr22	0.03023	Down
FOS	chr14	0.000558	Down
MT1JP	chr16	0.020193	Down
HIST2H2AA4	chr1	0.004303	Down
HIST2H2AA3	chr1	0.004311	Down
HSPA6	chr1	0.003029	Down
KLHL24	chr3	0.004291	Down
ITGAX	chr16	0.012826	Down
MT2A	chr16	0.020129	Down
ADSSL1	chr14	0.007323	Down
HSPA7	chr1	0.002476	Down
CCNG2	chr4	0.001532	Down
HILPDA	chr7	0.001728	Down
ACAP1	chr17	0.00539	Down
HMGA2	chr12	0.00064	Down
MYLIP	chr6	0.00057	Down
BCL6	chr3	0.001957	Down
EFNA3	chr1	0.003762	Down
RGS2	chr1	0.005095	Down
GIPR	chr19	0.008714	Down
MSMO1	chr4	0.002055	Down
MT1G	chr16	0.00146	Down
HMGCS1	chr5	0.001108	Down
MIR4742	chr1	0.01769	Down
MIR4674	chr9	0.026025	Down
RGS1	chr1	0.001476	Down
ACSS2	chr20	0.002753	Down
EGR1	chr5	0.002162	Down
SLC6A8	chrX	0.007646	Down

IZUMO4	chr19	0.000696	Down
STARD4	chr5	0.00215	Down
ADM	chr11	0.002677	Down
CREBRF	chr5	0.000385	Down
MT1X	chr16	0.001152	Down
ALDOC	chr17	0.006382	Down
PCSK4	chr19	0.000366	Down
HIST1H2AC	chr6	0.001582	Down
SAT2	chr17	0.000405	Down
MAFF	chr22	0.000416	Down
MIR4639	chr6	0.005829	Down
HIST2H2BE	chr1	0.001168	Down
DACT3	chr19	0.000162	Down
ENO2	chr12	0.003384	Down
HIST1H1C	chr6	6.45E-05	Down